

A. Elsenaar  
 National Aerospace Laboratory NLR  
 Anthony Fokkerweg 2  
 Amsterdam  
 The Netherlands

### Abstract

Testing laminar airfoils or wings in the wind tunnel, entails some specific experimental problems. These problems are discussed in the paper using the (limited) experience of laminar flow tests made in the High Speed Wind Tunnel HST of NLR. Special measurement techniques are required, like infrared imaging for transition detection and fast continuous wake rake traverses, for detailed drag assessment. Premature transition due to contamination of the airfoil surface appears to be a problem. It is unlikely that the transition location in flight will be duplicated in the wind tunnel due to flow quality and Reynolds number differences. Therefore a methodology is discussed to extrapolate the wind tunnel test result to flight conditions.

### 1. Introduction

The exploitation of laminar flow to reduce drag and hence improve the aerodynamic efficiency of aircraft, has been a challenging perspective since the thirties<sup>(1)</sup>. The interest in laminar flow shows peaks and valleys with renewed attention during the last decade. It is one of the few areas in the aerodynamic field with large potential benefits. Moreover, with improved manufacturing technologies, very smooth surfaces are now within reach. Recent activities in laminar flow technology have generally been concentrated on the development of linear stability theory (to provide better guide lines in the empirical art of transition prediction), flight experiments (to calibrate transition prediction methods and to investigate the feasibility of laminar flow wings under operational conditions) and the design of laminar airfoil sections and wings. Also, significant progress has been made in measuring techniques to probe the laminar boundary layer and to locate the transition location.

Next to theory and flight tests, wind tunnels play an essential rôle in the development of aircraft. The number of publications on wind tunnel investigations of laminar flow configurations appears to be somewhat limited, especially for the transonic regime. This is probably related to practical problems in laminar flow testing. This paper will discuss some of these problems, partly based on (limited) experience with laminar flow testing in the high speed wind tunnel HST of NLR. New experimental techniques are required to measure the transition location and the drag in sufficient detail but this can be done. It is of more concern that the quality of the flow (in terms of noise, turbulence, contamination) in a wind tunnel will be, generally speaking, less than

what is met at flight conditions. This effects the transition location. Since transition is also known to be very sensitive to Reynolds number variations, the difference between the tunnel and flight Reynolds number makes it even more difficult, if not impossible, to simulate in the wind tunnel the extent of laminar flow for flight conditions. Will it be possible to develop a methodology to simulate or extrapolate wind tunnel test results of laminar flow configurations to flight conditions? Some arguments related to this question will be discussed in the second part of this paper.

### 2. The tunnel environment

#### 2.1 Natural transition

The results that will be discussed in this paper, have been obtained in the transonic wind tunnel HST of NLR with test section dimensions of  $1.6 \times 2 \text{ m}^2$  (Fig.1). To increase the Reynolds number, the tunnel can be pressurized up to 4 bar at Mach=.5 and 2 bar at Mach=.8. Maximum Reynolds numbers based on chord length are approximately 3.5, 8 and 12 million at Mach=.8 for full model, half model and two-dimensional configurations respectively. The possibility to vary the Reynolds number has contributed significantly to the understanding of Reynolds number effects for conventional (fully turbulent) airfoils and wings<sup>(2,3)</sup>.

During windtunnel tests of more conventional designs, significant regions of laminar flow are often observed on the model, depending on the specific flow conditions. For the evaluation of test data from different wind tunnels, the ambiguity in natural transition location due to tunnel flow quality is a source of uncertainty. For this reason Dougherty and Fischer made<sup>(4)</sup> systematic measurements on a 10 degree cone. They observed a correlation between the noise level and the transition location. Although later studies(e.g.5) indicated that the relation between transition and disturbances in the tunnel flow is far more complex, the noise level, expressed as  $C_p$ -RMS still provides a first indication of the quality of the tunnel flow. The relatively low value for the HST (Fig.2) can be attributed to a very high contraction ratio (1:25) and the use of slotted instead of perforated walls in the test section. Part of the noise is generated by the model support: when removed a significant reduction in noise level results (Fig.3). Also, it has been reported<sup>(6)</sup> that support beams for wake rakes effect the transition location, a detail in measuring techniques that deserves more attention.

For an accurate prediction of the natural transition location the correlation with the noise level is far too simple. At present, the most accurate method is believed to be a correlation with the amplification factor  $N$  at the observed transition location as calculated from linear stability theory. Such a correlation is presented in Figure 4 for the HST, using measured transition locations on a two-dimensional laminar airfoil. The  $N$ -values have been taken from stability calculations with the (compressible) COSAL code<sup>(7)</sup>. At a low Mach number a  $N$ -value of 10 to 12 compares reasonably well with observations in the low speed wind tunnel DNW that appeared to be similar to the values observed in flight<sup>(8)</sup>. At the higher Mach number of .65 values between 6 and 9 are obtained. Unfortunately, there is no consensus on typical  $N$ -values at transonic conditions. Stability theory suggests a favourable effect of compressibility on transition (see also Fig.20), but the actually observed values in flight at transonic conditions range between roughly 6 and 12<sup>(9)</sup>. Figure 4 also suggests a decrease in the critical  $N$ -value with increasing Reynolds number. Again, it is not clear if this is due to an increased disturbance level at higher Reynolds numbers or that such a decrease in  $N$  will also occur at (ideal) flight conditions. In any case, the range of observed  $N$ -values suggests that the noise level in the HST is sufficiently low to guarantee appreciable regions of laminar flow.

## 2.2 Transition due to contamination

In Figure 5 an infrared picture is presented of a two-dimensional airfoil as measured in the HST at a chord Reynolds number of  $13.5 \times 10^6$ . Due to impact on the model of particles in the flow, disturbances are created on the model surface that trigger transition. As Figure 6 indicates, a single roughness element on the airfoil surface causes already a significant spanwise variation of the wake drag. The spanwise wake drag variation that corresponds to Figure 5 is presented in Figure 7. Due to the contamination of the airfoil all signs of a laminar region are eventually lost in the airfoil wake. This appears to be a general problem in laminar flow testing, although not often reported. In<sup>(10)</sup> examples are shown of oilflow patterns, that indicate at high Reynolds numbers the occurrence of turbulence wedges. Problems with surface contamination have also been reported in<sup>(6)</sup>.

Surface roughness effects provide a "by-pass" to the process of natural transition. A commonly used criterion to estimate the allowable roughness height is based on a "roughness Reynolds number" defined by:

$$Re_k = U_k \cdot k / \nu_k$$

with  $k$  = the height of the roughness element and  $U_k$  and  $\nu_k$  respectively the velocity and the kinematic viscosity in the (undisturbed) boundary layer at a distance  $k$  from the wall. Transition occurs when the roughness Reynolds number exceeds a critical value of about 625 for three-dimensional and about 100 for two-dimensional disturbances (this corresponds roughly to a factor of 2.5 in

critical roughness height). Experiments made at NLR<sup>(11)</sup> confirm this relation for a favourable pressure gradient. Small disturbances have also been applied intentionally near the leading edge of a two-dimensional airfoil in the HST (Fig.8). Critical values of about 800 have been observed (Fig.9), higher than expected in view of the two-dimensional nature of the disturbances (circular pieces of thin adhesive tape). The steep pressure gradient in the nose region of the airfoil or compressibility effects might have been responsible for this high value.

An analysis of the impact pattern on the airfoil nose for one of the earlier tests indicated a rather even distribution (Fig.10) suggesting that the particles are evenly distributed in the flow and follow straight trajectories even close to the airfoil nose. The counting was done after three days of testing and the large number of disturbances is not very comforting, although most disturbances are too small to be effective. These results prompted a more systematic investigation into the origins of the contamination problem. To this end a "particle collector" has been installed in the diffuser. This contraption is basically a small open duct with a removable aluminum plate and a filter at the end such that the flow is not completely blocked. At the end of each day the impact craters on the plate are counted whereas the particles collected in the filter can be analyzed. From these early recordings it appeared that the number of impacts increased drastically when the tunnel was pressurized. Better filters were installed in the air supply line, whereas air-inlet and blow-off pressure lines were separated. Also special procedures are followed to pressurize the wind tunnel. Many disturbances in the flow appeared to be man-made like small quantities of oil, plasticine, adhesive tape, rubber compound etc. that originated from the model or model related activities. Special procedures are now followed to reduce this part of the problem. Due to these actions the contamination has been reduced significantly but at high tunnel pressures (Reynolds numbers) long running times are still problematic.

A simple argument helps to understand the cause of the persistency of this problem. When  $N$  particles per  $m^3$  are present in the tunnel flow, the number of impacts  $n$  per meter span follows from:

$$n = N \cdot U \cdot T \cdot c / c$$

with  $U$  the free stream velocity,  $T$  the total running time and  $t/c$  the thickness to chord ratio of the airfoil. Even for a very low number of  $10^{-3}$  particles/ $m^3$  25 impacts will occur over a meter span after 30 minutes of testing ( $U=200$  m/sec,  $c=.5$  m,  $t/c=.15$ ). By the same argument partial filtering of the tunnel flow is likely to be quite effective and this will be tried in the near future.

## 2.3 Instrumentation

In view of possible contamination of the airfoil, it is essential to have an overall view during the execution of the test of the transition pattern on the wing. This is also required for an analysis of the aerodynamic characteristics.

Transition detection by means of the infrared technique (Fig.5,8) is well proven by now (see Fig.11 taken from (12)) and provides a good solution to this problem. At low Mach numbers when the temperature differences are small this technique is somewhat problematic. But when the tunnel is equipped with a cooling system (as is the case for the HST) use can be made of temperature transients, enabling the application of this technique also at low speeds. A disadvantage is that the model has to be provided with a thin layer of insulating material. An epoxy insert with a thickness of about 3 mm has been used on two-dimensional models. A double layer of PVC-foil ( $\approx .2$  mm thick) however, appeared to be sufficient as well and can be applied, with some care, on metal models. Dornier GmbH has made half model test with a wing of carbon-fiber-epoxy construction around a metal core and such a model is of course ideally suited for the application of the infrared technique.

Another experimental problem is the possibility that pressure holes trigger transition, at least at high Reynolds numbers (13). It has been argued that this is not caused by the disturbance of the hole itself, but by in- and outflow of air from the pressure tubing. According to the NLR experience .25 mm holes do not present a problem, even at the highest tunnel Reynolds numbers. However, this experience is limited to (almost) two-dimensional flows without cross-flow instabilities. It is nevertheless still often practice to locate pressure holes outside critical regions of laminar flow. This is a problem since rather accurate pressure distributions are required for the calculation of the laminar boundary layer development and the subsequent stability analysis as will be discussed below. It is felt that the possible effect of pressure holes on transition requires more attention.

Drag reduction is the main aim of laminar flow technology. Drag can be measured in a conventional way with balances. Since detail is lost in this way a permanent observation with the infrared technique is essential to observe the (unwanted) occurrence of turbulent wedges and (possibly) to correct for these effects if the wing is slightly affected. For the evaluation of a laminar flow design more detailed information will be required. This can be obtained by traversing a wake rake some distance behind the trailing edge. The use of a fast electronic pressure scanning system (EPS) is of great advantage here. Details of the application of this technique in the HST environment can be found in (14). It is sufficient to note here that the local wake drag (viscous and wave drag) is obtained from a continuously traversing wake rake by intergrating both in time and space. One complete scan over a span of 1 m can be made in 100 seconds. A typical example of the repeatability of the drag measurements is shown in Figure 6. In this case three scans (with various traversing speeds) have been made behind the laminar flow region of a two-dimensional airfoil (a disturbance has been fixed intentionally on the model nose in this case). Figure 12 shows an isobar plot of total pressure losses behind a half model wing tested in the HST. In this particular incidence, the inner wing has laminar flow on both surfaces whereas the outer wing is laminar on the upper surface only. Note

also the wavy-like character of the total pressure losses in the wake.

### 3. The Reynolds number problem

#### 3.1 General remarks

Figure 13 shows the (wake)drag of a laminar airfoil as a function of the incidence  $\alpha$  for three Reynolds numbers of 6.7, 9.6 and  $13.2 \cdot 10^6$  respectively. These results have been obtained in a continuous incidence sweep with the above discussed EPS system. The figure clearly illustrates the significant effect of a Reynolds number variation on the extent of the laminar drag bucket. It suggests that at a Reynolds number of 30 million (typical for a medium range transport aircraft) only a small low drag region would have left. But this is not necessarily the case: the flow quality in the wind tunnel environment might be such that the extent of laminar flow is underpredicted. These two elements, the Reynolds number gap and the influence of the flow quality on the transition location constitute the two basic problems in the extrapolation from windtunnel to flight. In this and the following sections some aspects of this problem will be presented to stimulate further discussion.

The "Reynolds number problem" for conventional (turbulent) aircraft has been dealt with extensively (1,2). In these references a distinction is made between direct and indirect Reynolds number effects (Fig.14). Direct Reynolds number effects are defined as the variation of viscous flow phenomena (like transition location, separation, viscous drag) with Reynolds number for a "frozen" pressure distribution. Indirect Reynolds number effects are related to changes in the pressure distribution (e.g. variations in shock strength and position, effecting wave drag, changes in incidence or pitching moment at constant lift) as a result of changes in the viscous boundary conditions on the airfoil surface resulting from the direct Reynolds number effect. Direct and indirect Reynolds number effects are closely connected due to so called "strong viscous flow coupling", but the distinction is useful for the understanding of the basic phenomena. Examples of both effects for laminar airfoils will be discussed in the next sections.

#### 3.2 Direct Reynolds number effects

The variation of the transition location (for a fixed pressure distribution) is a typical example of a direct Reynolds number effect. Since it depends on the signature of the pressure distribution one might expect that also the way in which the direct Reynolds number effect manifests itself, depends on the type of pressure distribution. In Figure 15 three different types of pressure distributions are schematically depicted. A good example of the types "A" and "B" (Fig.16) can be observed on respectively the upper and the lower surface of the laminar airfoil for which the drag variation was already shown in Figure 13. The corresponding transition point variations as observed in the wind tunnel at three different Reynolds numbers are presented in Figure 17. Type "A" represents a case where the location of the transition point changes gradually with incidence, whereas for type "B" an almost discon-

tinuous shift in transition location is noticeable. The type "C" pressure distribution (Fig.18), is typical for transonic conditions. The transition is caused by the steep pressure gradient at the shock location and the direct Reynolds number effect on the transition location is absent, provided that the pressure gradient in front of the shock is sufficiently favourable not to cause transition ahead of the shock.

The direct Reynolds number effect on the transition location can be estimated with stability theory. An illustration is given in Figure 19 where results of COSAL calculations in terms of the amplification factor N for two lift coefficients and two Reynolds numbers are shown. Similar results for the other two types of pressure distributions have been indicated schematically on the right side of Figure 15. Starting from measured pressure distributions at wind tunnel conditions, these calculations can provide estimates for the direct Reynolds number effect on the transition location, and hence the extent of the laminar flow bucket, as also indicated in Figure 15. The accuracy of such a prediction will depend critically on the reliability of the N-value method. Hence, extensive N-value correlations for flight conditions are indispensable.

When the flow quality in the wind tunnel is sufficiently good, the laminar drag bucket will be larger in the windtunnel than in flight due to a favourable effect of a Reynolds number decrease on the transition location. In principle the flow quality (e.g. noise or turbulence level) can be exchanged against the Reynolds number such that the transition locations will be identical for wind tunnel and flight (see Figure 19 for an illustration) In practice this appears not to be very useful in view of the complex and unknown relation between flow quality and transition. Note that an increase in turbulence level to increase the effective Reynolds number for windtunnel tests has also been suggested for conventional aircraft testing<sup>(15)</sup>, though on different arguments.

It is clear from this discussion that, in general, the natural transition location in flight will not be reproduced in the wind tunnel. Hence, a reliable transition prediction method is essential, not only for the design of laminar flow aircraft but also in a methodology to extrapolate wind tunnel results to flight conditions. Unfortunately, the universal validity of a critical N-value is today still very much an open question. In view of this uncertainty, it might be of advantage to correlate critical N-values for the usual range of wind tunnel test conditions as well. This correlation can be of the form:

$$\delta N_{\text{tunnel}} = N_{\text{flight}} - N_{\text{tunnel}} = \text{function} \\ \left( \frac{Re_{\text{tunnel}}}{Re_{\text{flight}}}, \text{tunnel flow quality} \right)$$

Such a correlation can be established by testing identical airfoil shapes in the wind tunnel and in flight (e.g. from wing glove flight tests).

The search for such a correlation might contribute to a better understanding of the limitations of the N-value method. Figure 4 suggests that the critical N-value decreases with increasing Mach number and, to a lesser extent, with increasing

Reynolds number. Since corresponding flight tests are not available for this case, it can not be decided if this variation is caused by a tunnel effect or reflects a more basic phenomena that is also present at flight conditions. The answer to this question is of interest not only for the windtunnel but also for flight. If such a correlation can be established the wind tunnel measurements may have some kind of predictive value for the transition location in flight. They are also required to analyze and understand transition point variations (e.g. with incidence) observed in the wind tunnel tests. Such variations can be due to unexpected pressure peaks or pressure gradients in the design, that might be unwanted in flight.

One final remark should be made here. It is now common practice to derive critical N-values from linear stability theory. But the N-value can be defined and calculated in different ways (see e.g. Fig.20) and there is no consensus at present which method gives the best representation of the actual transition process. This is of minor importance for one particular type of application but it prohibits a general exchange and build-up of experience. It seems to be essential that the aerodynamic community agrees on a standard method to define the critical N-value.

### 3.3 Indirect Reynolds number effects.

In section 3.2 the direct Reynolds number effect defined as the change in viscous effects for a "frozen" pressure distribution has been discussed. However, the pressure distribution itself is influenced to some extent by the boundary layer development. This variation in pressure distribution, defined as the indirect Reynolds number effect, represents a complicating factor in the Reynolds number problem for laminar airfoils.

A variation in boundary layer development due to transition point variations and/or Reynolds number changes causes a lift loss and a related variation in pitching moment. It is the cause of large non-linear variations in the lift and pitching moment curves for laminar flow airfoils as illustrated in the figures 21 and 22. The lift and pitching moment in this case was obtained from a pressure integration and the pressure holes might have influenced the transition location at the pressure section. For the lowest Reynolds numbers the flow is believed to be laminar up to 60 % chord for lift values between roughly 0.1 and 0.7. At the highest Reynolds number contamination of the airfoil surface has decreased the extent of laminar flow such that the result is more similar to a case with forward transition. Apart from this experimental difficulty, the figures illustrate significant non-linear effects due to transition point variations. Since the viscous losses depend on the Reynolds number, a change in Reynolds number will affect these variations. This kind of non-linear behaviour in the aerodynamic characteristics is of some concern for the application of laminar airfoils from the point of view of stability and control.

The Reynolds number effect to be discussed is related to a coupling between the natural transition location and the change in pressure distribution due to the indirect Reynolds number effect.

Figure 23 shows the pressure distribution of a laminar airfoil at two Reynolds numbers. The boundary layer was laminar up to about 60 % of the chord on upper and lower surface. Since the boundary layers are thin, the pressure distribution is hardly affected by the Reynolds number change. Figure 24 shows two pressure distributions for the same airfoil both at a Reynolds number of 9.5 million. In one case the flow was laminar over the forward part of the airfoil, in the other case premature transition occurred due to contamination of the airfoil in the wind tunnel. The change in pressure gradient over the front of the airfoil should be noted here. In that particular design, the pressure gradient over the rear of the airfoil was such that trailing edge separation occurred (at low tunnel Reynolds numbers) when the boundary layer was fully turbulent as can be seen from the pressure distribution.

The example illustrates a coupling between the transition location and the pressure distribution. Such a coupling might also occur for Reynolds number variations at conditions close to trailing edge separation. When the Reynolds number increases, the natural transition location will move forward (for type "A" pressure distributions), thereby increasing the extent of the trailing edge separation and (through the indirect Reynolds number effect) decreasing the pressure gradient over the front of the airfoil. This in turn will move the transition point further forward causing more trailing edge separation. The loss of lift that is related to this indirect Reynolds number effect, will be more severe when the boundary layer at the trailing edge is closer to separation. This can happen for conditions at "the flank of the drag bucket" where (for the upper surface) the transition moves upstream with increasing incidence. When the boundary layer is close to separation, a rotation of the "flank of the drag bucket" might be observed as depicted schematically in Figure 26. Such a rotation can also occur in the lift and pitching moment curves (Fig. 21 and 22).

There is no easy recipe to quantify this indirect Reynolds number effect. It will be more pronounced when the boundary layer is close to separation at the trailing edge. Such a situation might occur for a very critical laminar flow design, where some trailing edge separation is accepted in the off-design case of (unwanted) forward transition. Artificial boundary layer tripping might give some indication of the magnitude of the indirect Reynolds number effect. Also, theoretical tools will be needed to assess possible effects in more detail. Calculation methods that can accurately describe strong viscous/inviscid interactions in combination with detailed stability calculations are essential in this respect. Apart from the stability calculations, the situation is not very much different from more conventional airfoils that are close to separation at low tunnel Reynolds number.

### 3.4 From wind tunnel to flight; some thoughts

In <sup>(3)</sup> a methodology is described to treat Reynolds number effects for conventional aircraft in the transonic regime. In this section some ideas with respect to the possibility of such a methodology for laminar flow configurations will be described.

The prediction of the full scale aerodynamic characteristics from wind tunnel test results requires, among others, the "mapping" of the aerodynamic characteristics in the Lift-Mach number plane from wind tunnel to flight as a function of Reynolds number. Different flow regimes can be distinguished and figure 25 illustrates these regions tentatively for a laminar configuration. Three main regions have been indicated that differ in the maximum extent of laminar flow on the upper and/or lower surface. Region I is the laminar flow bucket with fully developed laminar flow (up to a steep pressure gradient) on both the upper and the lower wing (or airfoil) surface. In this region the design point is located. The extent of this region increases with increasing Mach number since compressibility has a favourable effect on boundary layer stability. Moreover, at a sufficiently high lift and Mach number the pressure distribution changes from type "A" or "B" to type "C" characterized by a region on the upper surface with a favourable pressure gradient terminated by a shock wave (Fig. 18). For the two other regions II and III transition occurs at one surface near the leading edge. Region II with turbulent flow on the upper surface, will be encountered at higher lift values where transition will be caused by a pressure peak at the leading edge. In region III only the lower surface is turbulent as a result of a pressure peak on the lower surface at sufficiently low lift values. In between the regions I and II and I and III transitional regions are present where large transition point variations can be observed, either gradually (type "A") or discontinuously (type "B"). The picture might be more complex than the one shown here when the pressure distribution is such that for the regions II and III transition point variations also occur on the lower, respectively the upper surface.

As is recommended for "conventional" designs <sup>(3)</sup>, the testing of a laminar flow configuration will also start with a "transition free" and a "transition fixed" configuration. The latter is realized by artificially tripping the boundary layer at a location close to the leading edge. The fixed transition case represents a "worst case". It is a logical requirement that a laminar flow design has acceptable aerodynamic characteristics when the wing is severely contaminated (e.g. due to insect contamination or adverse weather conditions). Additional information is obtained from tests where transition is artificially fixed on either the upper surface or the lower surface. A comparison of aerodynamic data for the free, mixed free/fixed and fixed transition cases provides a first indication (for windtunnel conditions!) of the flow regions where laminar flow occurs (by evaluating drag results), and its effect on the overall forces, moments and pressure distributions (if measured). The latter provides a first indication of the severity of possible indirect Reynolds number effects.

After this an in depth study of the transition point variations is required for the transition free case. The infrared technique, possibly in combination with (fast) wake rake traverses provides such a detailed map of the transition phenomena. Based on an interpretation of these data a distinction can be made between flow conditions where the transition is predominantly caused by steep pressure gradients or shock waves

(likely to be Reynolds number insensitive) and conditions where gradual transition point variations occur. This is similar to distinguishing between type "A", "B" or "C" pressure distributions. Boundary layer stability calculations are required to establish if the observed transition point variations are in line with the predictions (for wind tunnel test conditions) and how the transition locations are likely to change for flight conditions (using the N-value correlations described in 3.2).

In the extrapolation methodology region I will be discussed first. The extrapolation for this region will be simplified when the conditions (in terms of the  $C_L$ -Mach number plane) cover in the wind tunnel a larger region than in flight. This situation is likely to occur when the turbulence level in the wind tunnel is sufficiently low. In section 2 it is shown that the critical N-values are not too distinct from the (usually quoted) values for flight. The difference in Reynolds number between wind tunnel and flight is likely to provide sufficient compensation in this respect. If this is not the case it might be advantageous to lower the Reynolds number in the wind tunnel. In other words: one should try to establish laminar flow in the wind tunnel for those conditions where it will also occur in flight. It is to be expected that the indirect Reynolds number effects are small for these conditions. The large extent of laminar flow keeps the boundary layer thin and trailing edge separation will not be critical (if it is critical the off-design case with fully developed turbulent flow is likely to be unacceptable). Therefore boundary layer computations will be sufficiently accurate to scale the drag from wind tunnel to flight in this part of the flight regime, however with a possible exception for the effects of laminar separation bubbles as to be discussed below.

Due to the steep pressure gradient that terminates the laminar flow area in region I, laminar boundary layer separation will occur. Although laminar separation itself is Reynolds number independent, the extent of the separation bubble is not, due to the Reynolds number effect on transition in the free shear layer at the edge of the bubble. At typical tunnel Reynolds numbers the bubble length can be of the order of 10 % chord. It has a (local) effect on the pressure distribution and possibly on the drag. When shock waves are present, as will be the case for type "C" pressure distributions, Reynolds number effects on laminar shock-wave boundary layer interaction should also be included. There is a distinct lack of knowledge in this area and fundamental and applied research seems to be required.

The scaling problem for the regions II and III, with turbulent flow on one of the two airfoil surfaces, is similar to the conventional <sup>(3)</sup> scaling problem (the laminar surface will hardly contribute to the Reynolds number effect). The Reynolds number effects might be severe for a critical design. Testing at the highest possible Reynolds number is of advantage. An indication of the severity of the Reynolds number effects can be obtained from Reynolds number sweeps if the tunnel can be pressurized, provided that the natural transition location at the "laminar" surface is not affected.

The most difficult regions of Figure 25 to deal with are the transitional regions between the regions I and II and I and III. Since the natural transition location will in general not be duplicated in the wind tunnel (for reasons described in 3.2), linear stability calculations have to be used in the extrapolation process. The prediction of the transition point variations in this region is critically dependent on the validity of the N-value correlation for flight conditions. Moreover, if indirect Reynolds number effects are strong, a situation that is likely to occur, an additional uncertainty will be introduced in the calculations. However, since the extent of the laminar flow in region I is likely to be larger in the wind tunnel than in flight (see above) artificial transition strips at the (predicted) flight locations might provide a good simulation of the indirect Reynolds number effect. A refined aft-fixation technique might even be attempted by locating the transition strip downstream of the estimated flight transition location such that the boundary layer thickness at the trailing edge at tunnel Reynolds numbers is comparable with the (predicted) thickness at the flight Reynolds number.

The procedure as outlined above is far from simple although there is some similarity with the conventional scaling problem. Like the aft-fixation technique for conventional Reynolds number scaling, the aerodynamic characteristics (like  $C_L$ - $\alpha$ ,  $C_L$ - $C_m$  and  $C_L$ - $C_D$ ) have to be reconstructed piece wise by "patching" different parts of the measured characteristics (sometimes, as for drag, with additional theoretical scaling) together. A new aspect is that the flight prediction critically depends on the reliability of the N-value correlation. It seems fair to remark that in any serious design of a laminar aircraft critical N-values have to be obtained from flight tests using a laminar flow glove with a similar type of pressure distributions as anticipated in the design. Additional correlations with wind tunnel test results for the same glove geometry are important for a validation of some aspects of the extrapolation methodology. The use of cryogenic windtunnels to match flight Reynolds numbers does not provide an adequate answer to the scaling problem since tunnel environmental effects (the contamination problem will be especially severe at high unit Reynolds numbers) will spoil the proper simulation of the flight conditions.

#### 4. Concluding remarks

Test techniques, notably the infrared technique for the measurement of the transition location and fast scanning traversing wake rakes for drag assessment, seem to be adequate for detailed investigations of laminar flow configurations in the wind tunnel. Contamination of the model surface due to the impact of particles in the flow presents a problem and requires further attention. The extrapolation of wind tunnel test results to flight conditions constitutes the most serious problem in wind tunnel testing, not only in view of the Reynolds number difference, but also because the transition process itself is likely to be influenced by windtunnel environmental effects like noise and tunnel turbulence. When these disturbing effects are sufficiently low to realize at least the same extent of laminar flow in the



wind tunnel as in flight a methodology can be developed to predict flight characteristics on the basis of wind tunnel tests. However, some essential elements in this methodology still have to be filled in, leading to the following recommendations:

- since the transition location in flight has to be derived from calculations, detailed correlations of the critical N-value as derived from linear stability theory are essential; these correlations should also be made for tunnel conditions;
- the value of these correlations will improve considerably if the aerodynamic community can agree on a standard method to calculate critical N-values;
- fundamental studies to improve the physical understanding of the relative success of stability theory to predict transition, including the effects of external disturbances, should be strongly supported;
- fundamental and applied research is needed to investigate the Reynolds number effects on laminar separation bubbles and laminar shock wave boundary layer interactions.

#### Acknowledgements

In writing this paper the author has drawn extensively from information provided by D. Rozendal, A.C. de Bruin en B. van den Berg of NLR who were also willing to read the manuscript and to give valuable comments. The author also wishes to thank Mr. Luck of DORNIER GmbH for his kind permission to use data from halfmodel test made for one of DORNIER's development projects. Finally, the permission of the Netherlands Agency for Aerospace Programs (NIVR) to use results from wind tunnel tests made under contract is greatly appreciated.

#### References

- 1 Roland, A.  
"Research Authorization 201", Appendix F from "Model Research, The NACA 1915-1958", The NASA History Series, NASA SP-4103
- 2 Elsenaar, A et al  
"Reynolds Number Effects in Transonic Flow", AGARDograph 303 (1988)
- 3 Laster, M.L.  
"Boundary layer Simulation and Control in Wind Tunnels", AGARD AR 224 (1988)
- 4 Dougherty, N.S. et al  
"Boundary Layer Transition on a 10-Degree Cone: Wind Tunnel / Flight Data Correlation", AIAA paper 80-0154 (1980)
- 5 Michel, U Froebel, E  
"Flow Unsteadiness in Three Low-Speed Wind Tunnels", in AGARD CP 429 (1987)
- 6 Dziomba, B Szodruich, J  
"Laminar Wing Testing Techniques in Wind Tunnel and Flight", International Congress on Instrumentation in Aerospace Simulation Facilities ICIASF'89; (not in conference proceedings)

- 7 Malik, M.R.  
"Finite Difference Solution of the Compressible Stability Eigenvalue Problem", NASA CR 3584 (1982)
- 8 Horstmann, K.H. Quast, A Redeker, G  
"Flight and Windtunnel Investigation on Boundary Layer Transition at Reynolds Numbers up to  $10^7$ ", ICAS-88-3.7.1
- 9 Berry, S.A. Dagenhart, J.R. Viken, J.K. Yeaton, R.B.  
"Boundary-Layer Stability Analysis of NLF and LFC. Experimental Data at Subsonic and Transonic Speeds", SAE Technical Paper Series 871859 (1987)
- 10 Eggleston, B Poole, R.J.D. Jones, D.J. Khalid, M  
"Thick Supercritical Airfoils with Low Drag and Natural Laminar Flow", J.Aircraft, Vol.24, No.6 (1987)
- 11 de Bruin A.C.  
"The Effect of Single Roughness Elements on Boundary Layer Transition in a Favourable Pressure Gradient", NLR CR 89095L (1989)
- 12 Rozendal, D  
"An Infrared Imaging Technique for Continuous Boundary Layer Transition Observation", NLR Memorandum AC-88-008U (1988)
- 13 Somers, D.M. Stack, J.P. Harvey, W.D.  
"Influence of Surface Static-Pressure Orifices on Boundary-Layer Transition", NASA TM 84492 (1984)
- 14 Elsenaar, A Rohne, P.B. Rozendal, D. Poestkoke, R.  
"Instrumentation Requirements for Laminar Flow Research in the NLR High Speed Wind Tunnel HST", Conference Proceedings of the International Congress on Instrumentation in Aerospace Simulation Facilities ICIASF'89 (1989); also NLR TP 89158L
- 15 Green, J.E.  
"On the Influence of Free-stream Turbulence on a Turbulent Boundary Layer, as it Relates to Windtunnel Testing at Subsonic Speeds", RAE TR 72201 (1972)

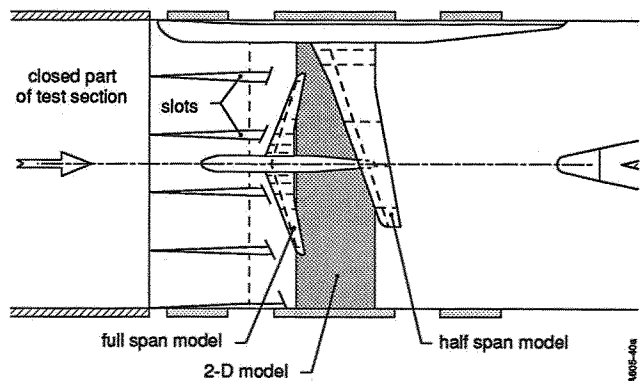


Figure 1 Various model configurations in the test section of the HST

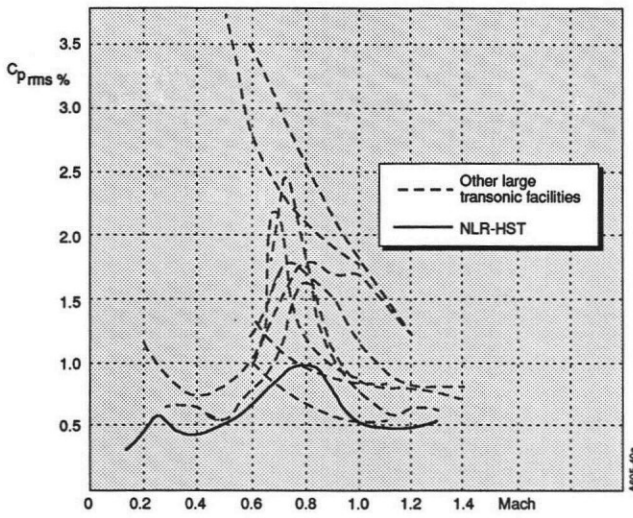


Figure 2 HST noise level compared with other large transonic facilities

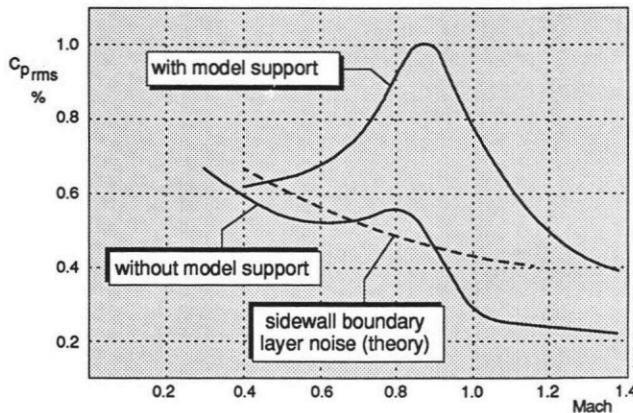


Figure 3 Effect on test section noise level of the removal of the model support

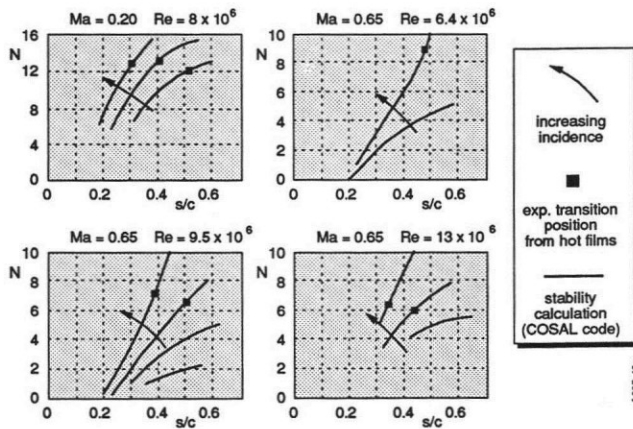


Figure 4 N-values as calculated for the measured transition locations on a two-dimensional airfoil in the HST (compressible COSAL code)

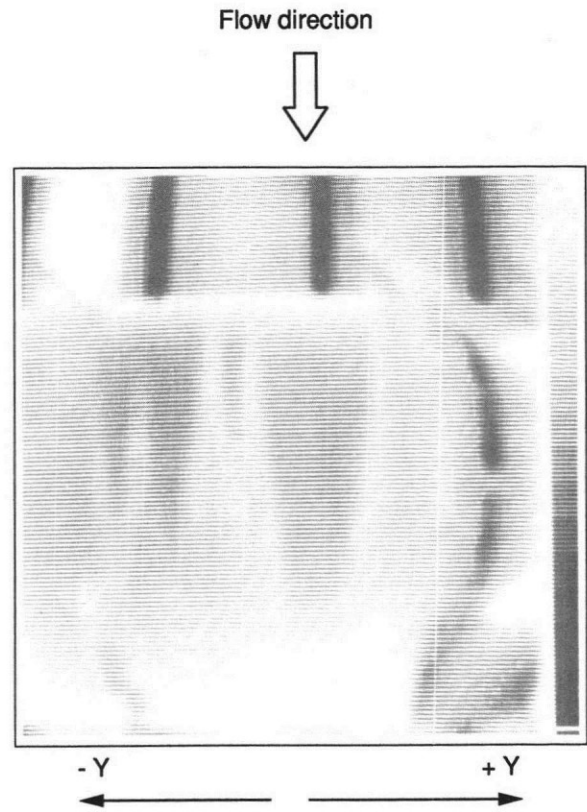


Figure 5 Infrared picture of contaminated airfoil (Mach = 0.65,  $Re = 13.4 \times 10^6$ ; see fig. 7 for corresponding wake drag)

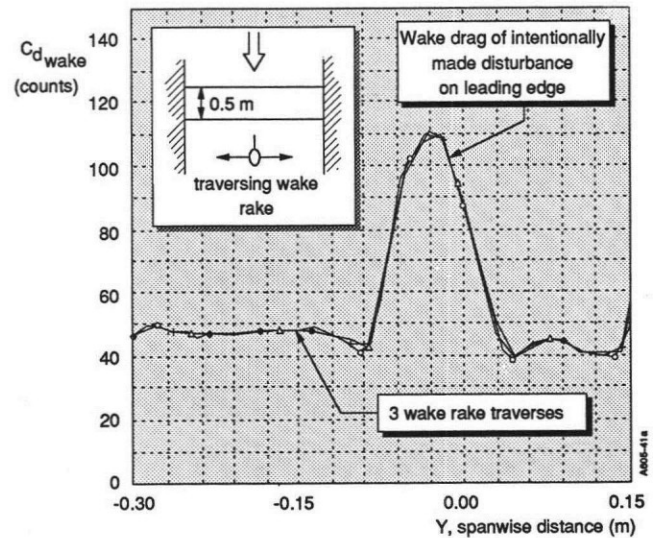


Figure 6 Spanwise variation of wake drag behind a two-dimensional airfoil with a single roughness element indicating repeatability of continuous wake rake traverses (Mach = 0.65,  $Re = 6.5 \times 10^6$ )



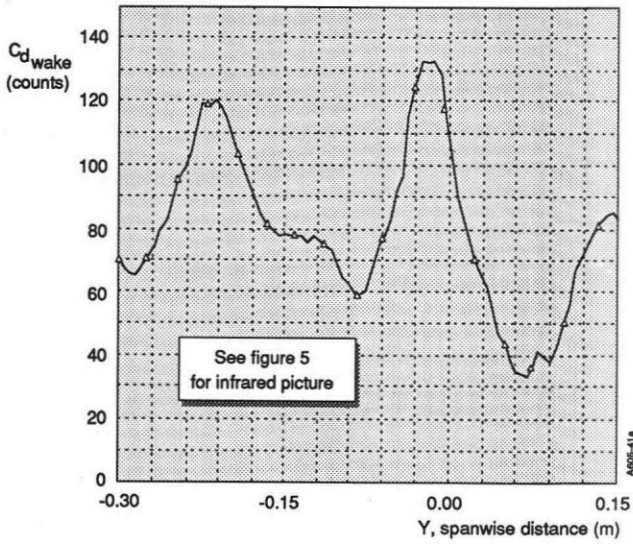


Figure 7 Spanwise wake drag variation for a contaminated airfoil (Mach = 0.65,  $Re = 13.4 \times 10^5$ )

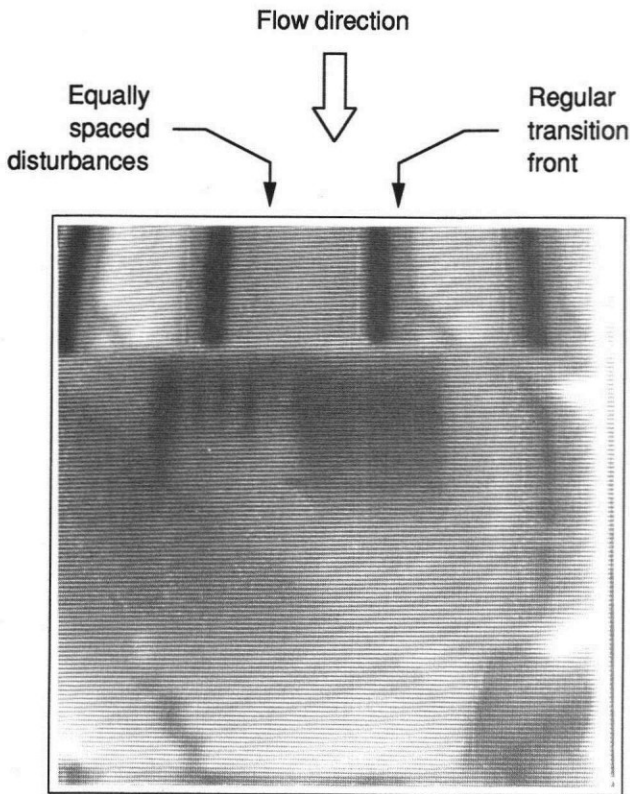


Figure 8 Infrared picture from a test to determine the critical roughness height at the leading edge of a laminar airfoil (Mach = 0.65,  $Re = 10 \times 10^5$ ; see fig. 9)

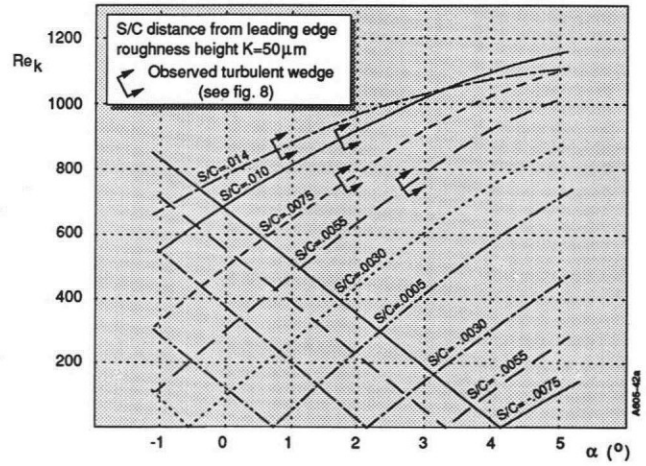


Figure 9 Reynolds number based on critical roughness height (intentionally applied disturbances in leading edge region) (Mach = 0.65,  $Re = 10 \times 10^6$ )

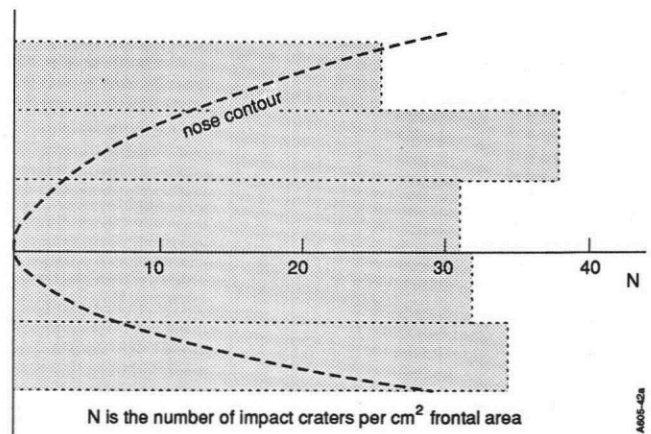


Figure 10 Density distribution of disturbances in the nose region of a two-dimensional laminar airfoil after three days of testing

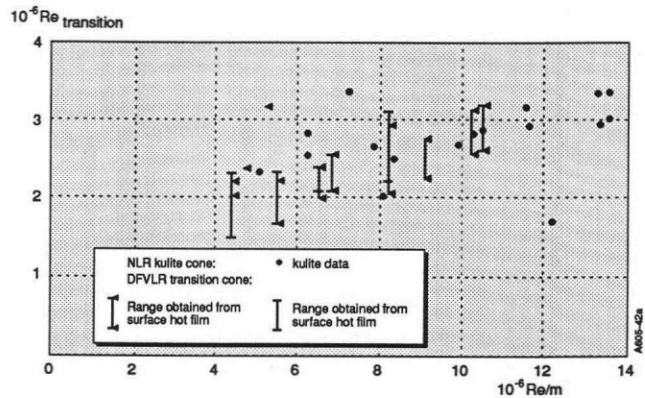


Figure 11 Comparison of transition locations measured by different methods

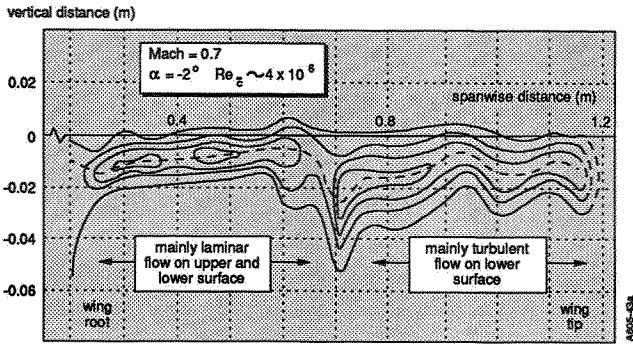


Figure 12 Isobar pattern of total pressure losses behind a half-model of a laminar wing (from a continuous wake rake traverse)

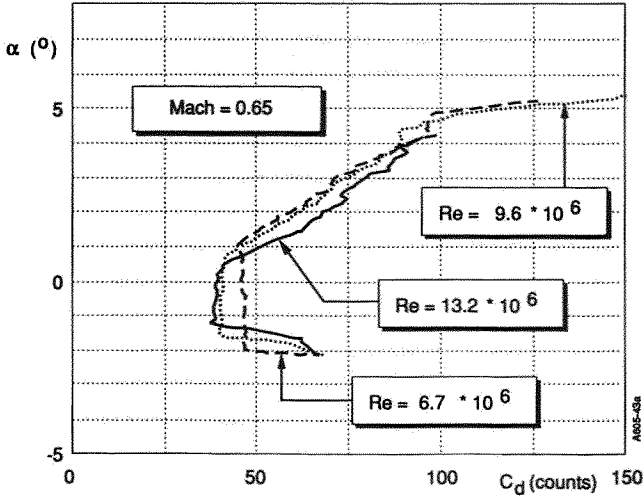
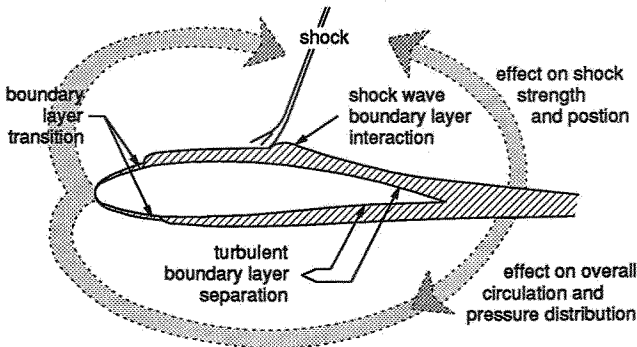


Figure 13 Effect of Reynolds number on the "drag bucket" of a laminar airfoil



→ Direct Reynolds number effect  
 ↗ Indirect Reynolds number effect

Characteristic	Dominant Re-number effect	
	direct	indirect
Lift and pitching moment		X
Viscous drag	X	
Wave drag		X
Drag divergence		X
Boundary layer separation	X	
Buffet boundary	X	X

Figure 14 Schematic representation of direct and indirect Reynolds number effects (from ref. 2)

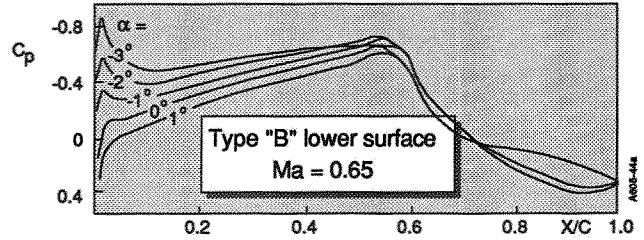
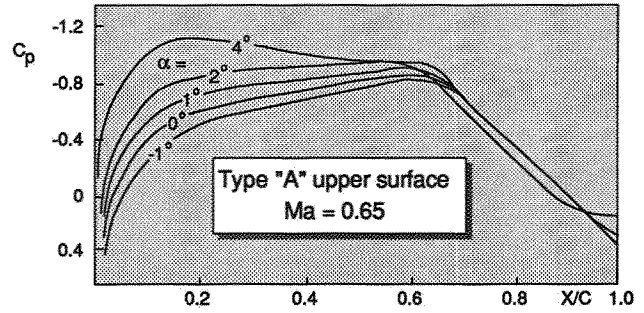


Figure 16 Examples of type "A" and "B" pressure distributions

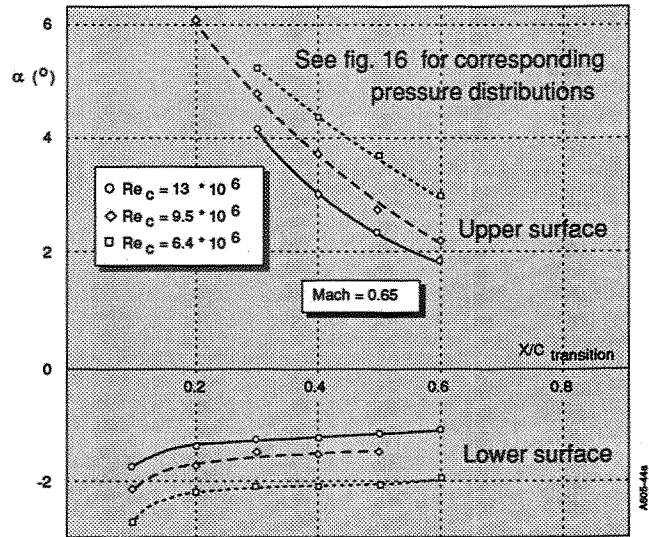


Figure 17 Illustration of the direct Reynolds number effect on the transition location for type "A" and type "B" pressure distributions (see fig. 16)

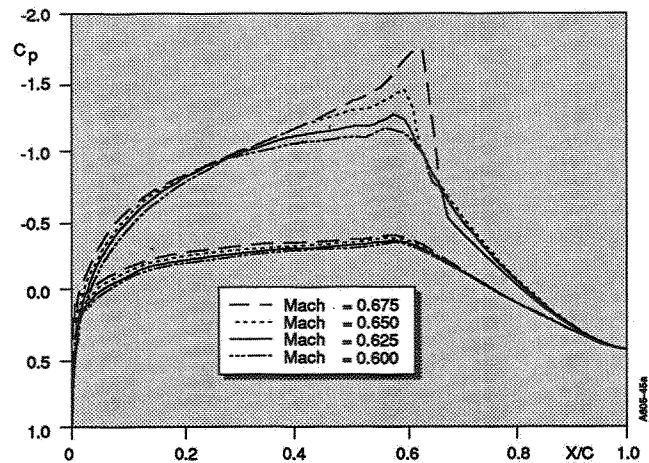
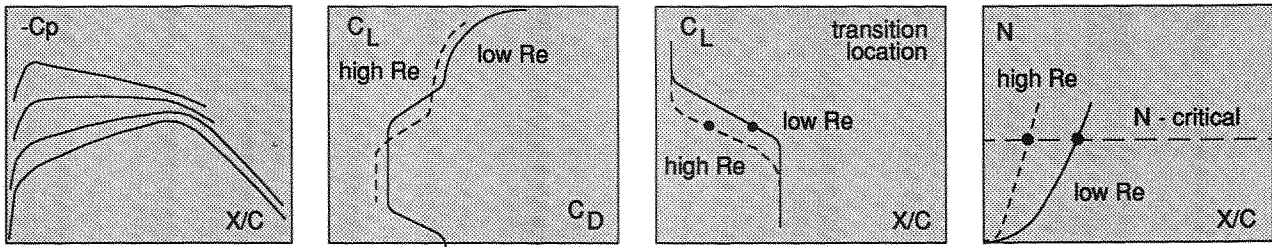
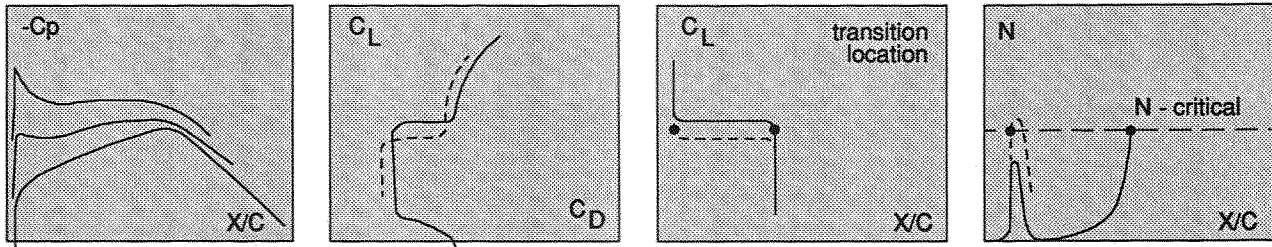


Figure 18 Development of type "C" pressure distribution with increasing Mach number

type "A"



type "B"



type "C"

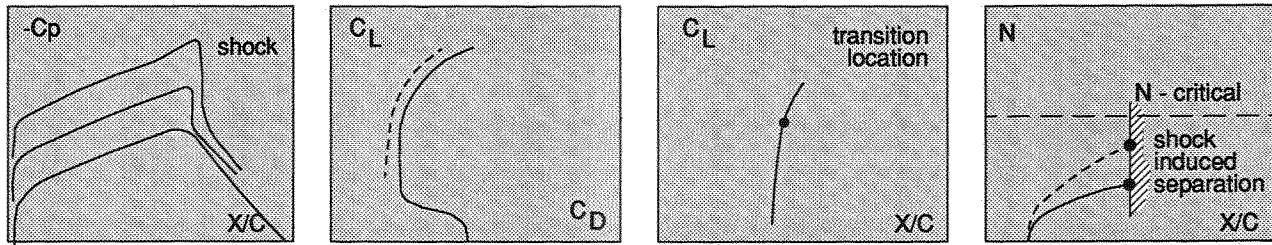


Figure 15 Various types of pressure distributions and related transition point variations with lift and Reynolds number

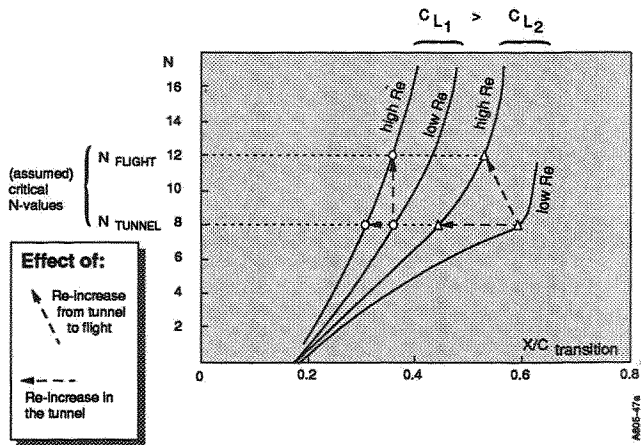


Figure 19 Possible equivalence of low Reynolds number, low N-crit. tunnel and high Reynolds number, high N-crit. flight conditions

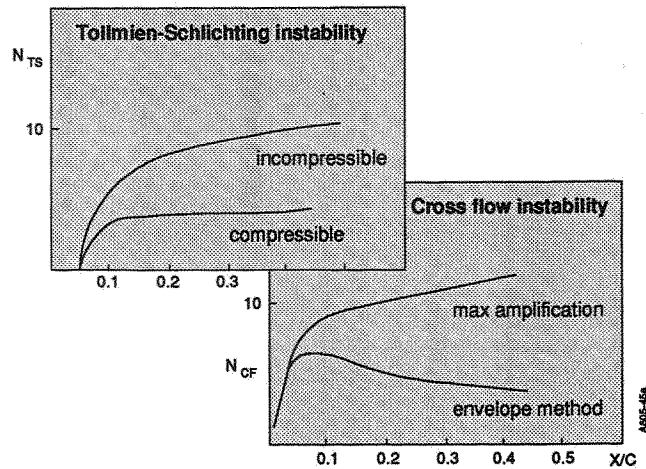


Figure 20 Examples of calculated N-values using various options of the COSAL code (Mach = 0.75, 20 deg LE-sweep)



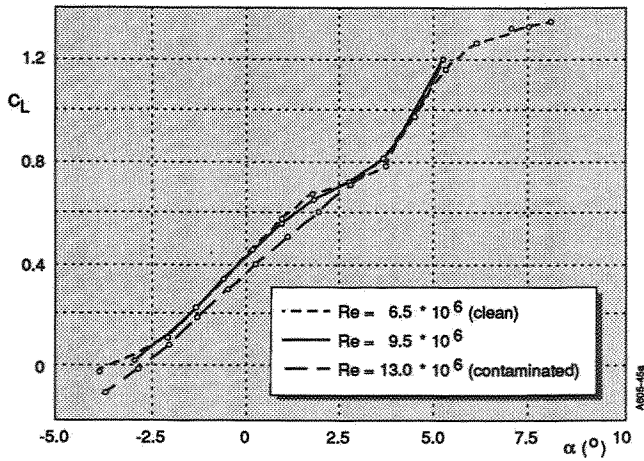


Figure 21 Effect of Reynolds number (and contamination) on pitching moment development for a laminar flow airfoil (Mach = 0.65)

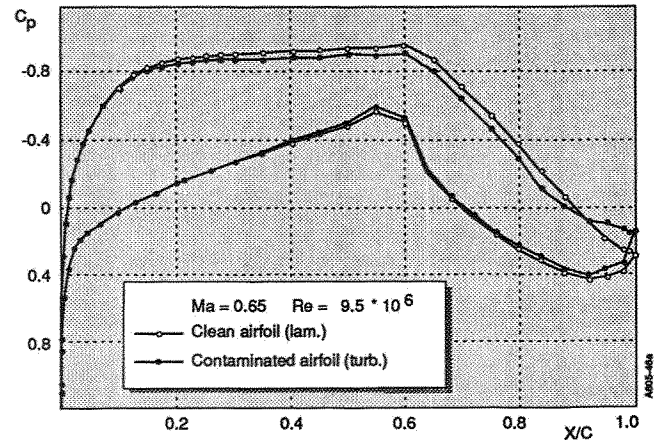


Figure 24 Change in pressure distribution due to contamination causing forward transition

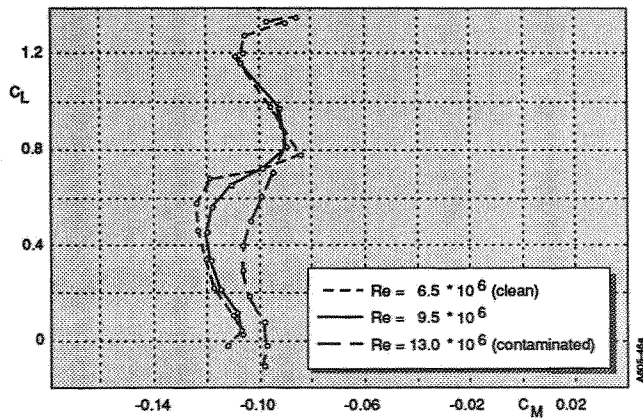


Figure 22 Effect of Reynolds number (and contamination) on pitching moment development for a laminar flow airfoil (Mach = 0.65)

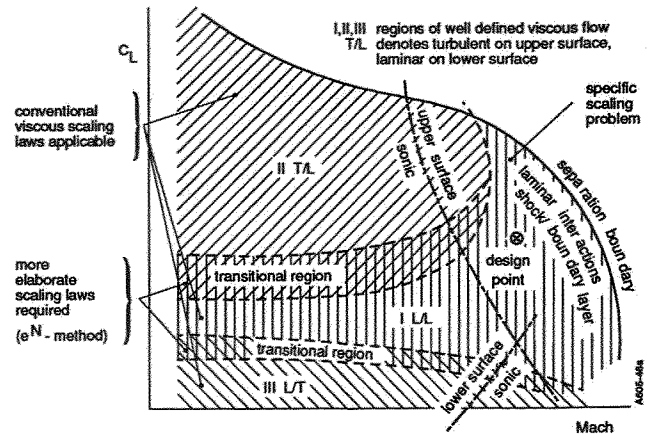


Figure 25 Various flow regimes relevant for a Reynolds number extrapolation methodology for laminar flow configuration

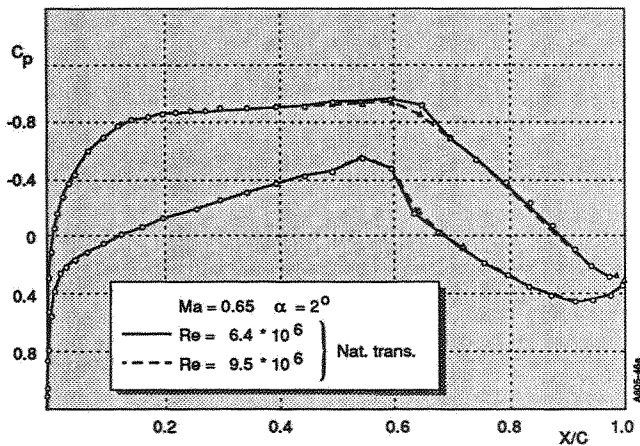


Figure 23 Effect of a Reynolds number variation on the pressure distribution with laminar flow up to 60% chord

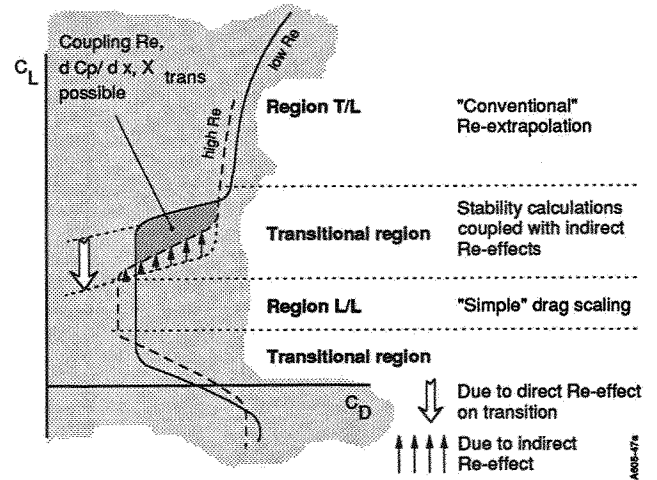


Figure 26 Summary of a Reynolds number extrapolation methodology